

*FINAL REPORT OF*

# **GENERATION OF PSEUDO CT IMAGE FROM MRI IMAGE OF SPINE**

*A Graduate Project Report submitted to Manipal Academy of Higher Education in  
partial fulfillment of the requirement for the award of the degree of*

## **BACHELOR OF TECHNOLOGY**

**In**

**Electronics and Communication Engineering**

*Submitted by*

**Shivam Kumar Sharma**

**170907044**

**Hritvik Kishore**

**170907150**

*Under the guidance of*

**Dr. Anitha H.**

**Professor**

**DEPARTMENT OF ELECTRONICS AND COMMUNICATION ENGINEERING**



**MANIPAL INSTITUTE OF TECHNOLOGY**

**MANIPAL**

*(A constituent unit of MAHE, Manipal)*

**MANIPAL-576104, KARNATAKA, INDIA**

**MARCH/APRIL 2021**

## CONTENTS

	Topic	Page Number
	<a href="#"><u>ABSTRACT</u></a>	
<i>Chapter 1</i>	<a href="#"><u>INTRODUCTION</u></a>	1
1.1	<a href="#"><u>General Discussion on Area of Work</u></a>	1
1.2	<a href="#"><u>Brief present day scenario with regard to the work area</u></a>	1
1.3	<a href="#"><u>Motivation to do the project work</u></a>	2
1.4	<a href="#"><u>The objective of the work</u></a>	3
1.5	<a href="#"><u>Target Specifications</u></a>	3
1.6	<a href="#"><u>Project Work schedule</u></a>	4
<i>Chapter 2</i>	<a href="#"><u>BACKGROUND THEORY</u></a>	5
2.1	<a href="#"><u>Chapter Summary</u></a>	5
2.2	<a href="#"><u>Project Specific Discussion</u></a>	5
2.3	<a href="#"><u>The summarized outcome of the literature review</u></a>	8
2.4	<a href="#"><u>Theoretical discussions</u></a>	11
2.5	<a href="#"><u>General analysis</u></a>	11
2.6	<a href="#"><u>Conclusions</u></a>	11
<i>Chapter 3</i>	<a href="#"><u>METHODOLOGY</u></a>	12
3.1	<a href="#"><u>Overview</u></a>	12
3.2	<a href="#"><u>Methodology</u></a>	12
3.3	<a href="#"><u>Tools used</u></a>	14
3.4	<a href="#"><u>Preliminary result analysis</u></a>	15
3.5	<a href="#"><u>Conclusions</u></a>	17
<i>Chapter 4</i>	<a href="#"><u>RESULT ANALYSIS</u></a>	18

4.1	<u>Overview</u>	19
4.2	<u>Result analysis</u>	19
4.3	<u>Significance of the result obtained</u>	22
4.4	<u>Deviations from expected results &amp; Justification</u>	22
4.5	<u>Conclusions</u>	22
Chapter 5	<u>CONCLUSION AND FUTURE SCOPE OF WORK</u>	23
5.1	<u>Brief summary of the work</u>	23
5.2	<u>Conclusions</u>	23
5.3	<u>Future scope of work</u>	23
	<u>REFERENCES</u>	25
	<u>PROJECT DETAILS</u>	26

## ABSTRACT

Magnetic Resonance-guided Radiation Therapy (MRgRT) is a promising approach to improving clinical outcomes for patients treated with radiation therapy. The roles of image guidance, adaptive planning, and magnetic resonance imaging in radiation therapy have been increasing over the last two decades. Technical advances have led to the feasible combination of magnetic resonance imaging and radiation therapy technologies, leading to improved soft-tissue visualisation, assessment of inter-and intrafraction motion, motion management, online adaptive radiation therapy, and the incorporation of functional information into treatment. MRgRT can potentially transform radiation oncology by improving tumour control and quality of life after radiation therapy and increasing the convenience of treatment by shortening treatment courses for patients.

This project focuses on the generation of Synthetic CT images from provided input MR Images. An accurate result can potentially add valuable substance to the field of Medical Imaging. Registration of MRI with patients' X-ray to date continues to be a non-trivial task due to the lack of a good correlation between the two.

To date, there are only two commercial synthetic CT software solutions that are available for MR-only planning for the prostate for clinical use. One of them is a classification-based method called MRCAT,<sup>1</sup> or MR for Calculating Attenuation, which is currently limited to a Philips MR scanner. The method uses a Dixon-based MR sequence along with a constrained shape model for bones to generate synthetic CT by assigning bulk HU for water, fat, and spongy and cortical bones. The method has been clinically implemented. The other method (MRI planner<sup>2</sup>) is scanner-independent and currently, CE is marked for clinical use in Europe. MRI planner uses a statistical decomposition algorithm for generating synthetic CT and has been evaluated for dosimetric accuracy within a multicenter/multivendor validation where accuracy was within 1% of CT-based plans.

A desirable Pseudo-CT image can dramatically solve the pre-existing conundrum of Registering MR with X-Ray Images and can hence be a great leap forward.

# CHAPTER 1

## INTRODUCTION

### *1.1 General Discussion on Area of Work*

The past decade has shown that magnetic resonance imaging (MRI) is increasingly being utilised in the radiation therapy setting not only for radiation therapy planning (RTP) purposes but also in the assessment of treatment response and MR-guidance therapy. Due to the ever-growing use of MRI in radiation therapy, more departments will inevitably be looking to move forward and use MRI as a complementary imaging modality in their RTP protocols or as a sole imaging modality in MR-only workflows. This project is primarily focused on the domain of Image-Guided Therapy which often involves registering different modalities of scans obtained from the patients.

Medical imaging comprises different imaging modalities and processes to image the human body for diagnostic and treatment purposes. It, therefore, plays an essential role in improving public health for all population groups. Medical imaging is frequently used in the follow-up of a disease already diagnosed or treated. Standard imaging type includes Computed Tomography (CT), Magnetic Resonance Imaging (MRI), X-Ray, Ultrasound. This project will be focusing on the first two.

CT imaging has been traditionally used as the primary source of image data in the planning process of external radiation therapy. In recent years, interests in replacing CT with MRI in the treatment planning process have grown rapidly. This is mainly because MRI is free of ionizing radiation and offers superior soft-tissue contrast that allows more accurate target and structure delineation.

### *1.2 Brief present day scenario with regard to the work area*

A crucial requirement for MR-only simulation and planning is the ability to perform dose calculation and patient positioning using MR images. A synthetic CT image is one created directly from an underlying base MR image through a method of tissue classification and subsequent assignment of CT Hounsfield number, which can then be used to describe the X-ray attenuation properties of the tissue.

The development of synthetic CT was spurred by the growth of PET-MR and, recently, MR simulators and MR-linacs. A systematic review of synthetic CT generation methods for an MR-only workflow has been recently reported. Regardless of the synthetic CT method used, the synthetic CT images should be thoroughly commissioned for their geometric and dosimetric accuracy before using them clinically for an MR-only workflow. Ideally, the synthetic CT generation method should be real-time, and, if possible, scanner and sequence-independent for wide adoption in the clinic. The methods for generating synthetic

CTs for MR-guided radiotherapy can be broadly classified into bulk density assignment, atlas-based, voxel-based, and hybrid Methods.

To date, there are only two commercial synthetic CT software solutions that are available for MR-only planning for the prostate for clinical use. One of them is a classification-based method called MRCAT,<sup>1</sup> or MR for Calculating Attenuation, which is currently limited to a Philips MR scanner. The method uses a Dixon-based MR sequence along with a constrained shape model for bones to generate synthetic CT by assigning bulk HU for water, fat, and spongy and cortical bones. The method has been clinically implemented. The other method (MRI planner<sup>2</sup>) is scanner-independent and currently, CE is marked for clinical use in Europe. MRI planner uses a statistical decomposition algorithm for generating synthetic CT and has been evaluated for dosimetric accuracy within a multicenter/multivendor validation where accuracy was within 1% of CT-based plans.

### *1.3 Motivation to do the project work*

#### *1.3.1 Brief importance of the work in the present context:*

In several cases, CT imaging is needed for the generation of digitally reconstructed radiographs (DRRs). Image co-registration errors between MRI and CT can be avoided by using MRI-only-based treatment planning. MRI-only radiotherapy aims to remove the planning CT from the workflow to eliminate this registration uncertainty. Additional support for the use of MRI-alone workflow is the lack of patient exposure to ionising radiation, the ability to also acquire a range of functional imaging sequences, and potential cost savings from the use of a single imaging modality.

Since electron density information can not be directly derived from the MRI, registering x-ray images to MRI data becomes difficult because of their fundamental difference in tissue contrast, and a method is needed to convert MRI data into CT-like data. Therefore CT imaging is needed for the generation of digitally reconstructed radiographs (DRRs).

#### *1.3.2 Shortcomings in the previous work/reference paper:*

**Bulk Density Approach:** This approach is not very accurate as tissue heterogeneity is ignored, and it is impossible to generate realistic digitally reconstructed radiographs (DRRs). Bone contouring would be required for DRR generation, and the use of an MRI simulation image would be needed as a reference for cone-beam CT guidance.

**Atlas Based Approach:** Pure atlas-based methods require accurate deformable image registration of atlas and patient MR images. It, however, can be difficult to accurately register a patient image with an arbitrary atlas, especially when there are large anatomical variations or pathological differences.

**Learning-Based Approach:** Accurate intra-patient alignment of MR and CT images is an important prerequisite and can become a bottleneck for developing accurate learning models. Misalignment in training data can cause inaccuracy as the model will be trained to make wrong predictions. Also, training requires a huge amount of data which may not be possible while working with medical images. Even training the model can take days or months.

### *1.3.3 The uniqueness of the methodology that will be adopted:*

The project successfully mimics the beam hardening artifacts which is a characteristic feature of CT images. The proposed method is simpler than previously reported approaches which require either acquisition of several MRI series or T2\* maps with special imaging sequences.

### *1.3.4 Significance of the possible end result:*

Image co-registration errors between MRI and CT can be avoided by using MRI-only-based treatment planning. Generating pseudo-CT images from MRI will inadvertently make the registration process much faster and will therefore facilitate the process.

### *1.4 The objective of the work*

The primary objective of the project is to generate synthetic-CT/pseudo-CT images from MRI images. The pseudo-CT image should have a good correlation to a corresponding CT image. Registering 3D CT or MR images to 2D X-ray images can help us to estimate the position and orientation of the patient's anatomy and is therefore very crucial during Image-Guided Therapy.

A variety of 2D–3D registration methods have been developed in the past of which most apply only for the registration of CT to X-ray images. However, for some applications, additional images providing the adequate soft tissue contrast may be of great value. Registration of X-ray to MRI data might provide such complementary soft tissue information which is absent in X-ray images.

However, registering X-ray images to MRI data is a non-trivial task due to the difference in tissue contrasts. Thus, in this project, we'll be focused on generating a pseudo-CT image from an input MRI, such that it will showcase a good intensity relationship with corresponding X-Rays.

### *1.5 Target Specifications*

The desired target pseudo-CT image must be able to highlight the bony structures distinctly compared to the muscular tissues. The characteristics of the output image must resemble those similar to the beam hardening artifacts seen in a CT image; such that it has a good correlation with a real CT image. The generated pseudo-CT will improve the process of MRI to X-Ray registration and would in turn facilitate image-guided therapy.

*1.6 Project Work schedule*

<i>January 2021</i>	<ul style="list-style-type: none"><li>○ Learning basics of medical imaging techniques</li><li>○ Literature Survey</li><li>○ Acquisition of training images</li><li>○ Preliminary Experiments</li></ul>
<i>February 2021</i>	<ul style="list-style-type: none"><li>○ Reading Research Papers related to pCT generation.</li><li>○ Preprocessing of training images.</li><li>○ Trying simple algorithms</li></ul>
<i>March 2021</i>	<ul style="list-style-type: none"><li>○ Finding out different algorithms for the pCT generation</li><li>○ Coding a few Python Scripts for obtaining raw data from DICOM images</li><li>○ Mathematical Modelling of obtained data</li><li>○ Reading Research Papers</li><li>○ Trying different algorithms for better result</li></ul>
<i>April 2021</i>	<ul style="list-style-type: none"><li>○ Generating a synthetic-CT image on basis of the modeling done</li><li>○ Analysis of the image generated</li><li>○ Documentation</li></ul>



## **CHAPTER 2**

### **BACKGROUND THEORY**

#### *2.1 Chapter Summary*

The project is a multidisciplinary project involving medicine, engineering, and physics, hence in this chapter, we will discuss the fundamental theories, principles, and terminologies used in these fields of sciences. The unit discusses a few radiology principles and aspects related to our project. Also, a literature review for the referred papers is provided to explain the inferences that were obtained from the given papers.

#### *2.2 Project Specific Discussion*

Our study is primarily focused on the Spine. The spinal cord is a long, fragile tubelike structure that begins at the end of the brain stem and continues down almost to the bottom of the spine. The spinal cord consists of nerves that carry incoming and outgoing messages between the brain and the rest of the body. In most adults, the spine is composed of 33 individual back bones (vertebrae). Just as the skull protects the brain, vertebrae protect the spinal cord. The vertebrae are separated by disks made of cartilage. The vertebrae and discs of cartilage extend the length of the spine and together form the vertebral column, also called the spinal column. The project results can be considered viable if the Spinal Columns' Vertebrae are visibly distinct compared to the soft tissues surrounding them.

One of the core themes of the project is the primacy of MRI compared to CT imaging. This is due to its advantage over CT in being able to detect flowing blood and cryptic vascular malformations. It can also detect demyelinating diseases. However, CT images are more desirable for Image Registration purposes due to their good correlation with X-rays. Hence, the need for replicating the beam-hardening artifacts of CT images becomes a trivial problem. Beam hardening is based on selective attenuation of lower energy photons.

Another crucial aspect related to a better understanding of the project lies in the Physics of MRI. MRI is based on the magnetization properties of atomic nuclei. A powerful, uniform external magnetic field is employed to align the protons that are normally randomly oriented within the water nuclei of the tissue being examined. This alignment (or magnetization) is next perturbed or disrupted by the introduction of an external Radio Frequency (RF) energy. The nuclei return to their resting alignment through various relaxation processes and in so doing emit RF energy. The emitted signals are measured and used to convert the frequency information contained in the signal from each location in the image plane to corresponding intensity levels in a matrix arrangement of pixels.

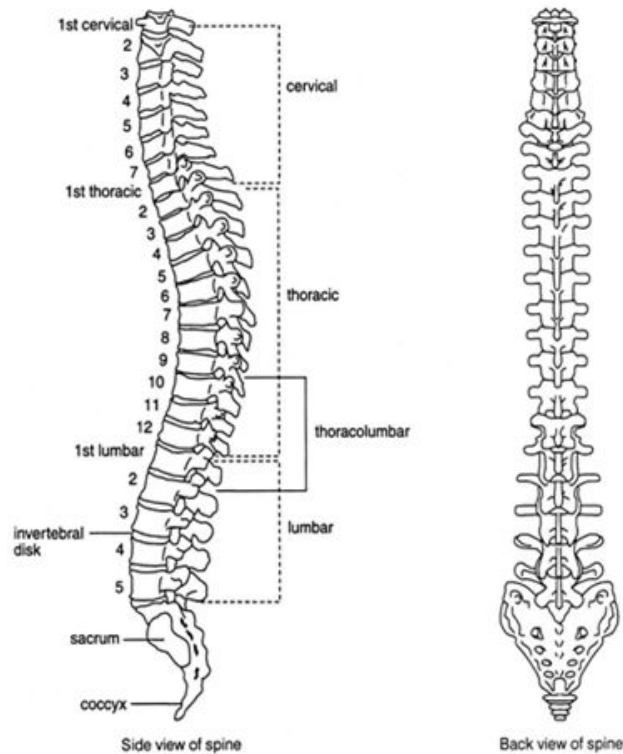


Figure 2.1: Spinal Column

By varying the sequence of RF pulses applied and collected, different types of images are created. Repetition Time (TR) is the amount of time between successive pulse sequences applied to the same slice. Time to Echo (TE) is the time between the delivery of the RF pulse and the receipt of the echo signal. Tissue can be characterized by 2 different relaxation times – T1 (longitudinal relaxation time) and T2 (transverse relaxation time).

The most common MR sequences are T1-weighted and T2-weighted. In T1-weighted images contrast and brightness of the image are predominantly determined by the T1 properties of tissue; and T2 properties for T2-weighted images.

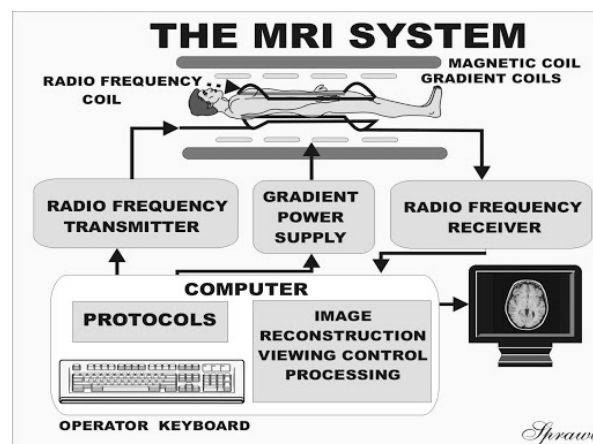


Figure 2.2: Process of Acquiring MR image

In general, T1 and T2-weighted images can be easily differentiated by looking at the CSF. CSF is dark on T1-weighted imaging and bright on T2-weighted imaging.

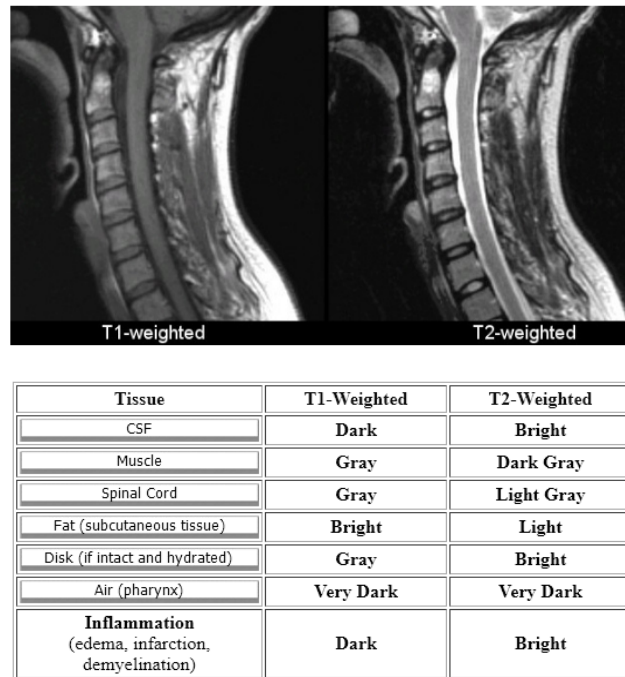


Figure 2.3: Comparison of T1 and T2 weighted images

A CT system consists of an X-ray source, rotary table, X-ray detector, and a data processing unit for computation, visualization, and data analysis of measurement results (see Figure 2.4).

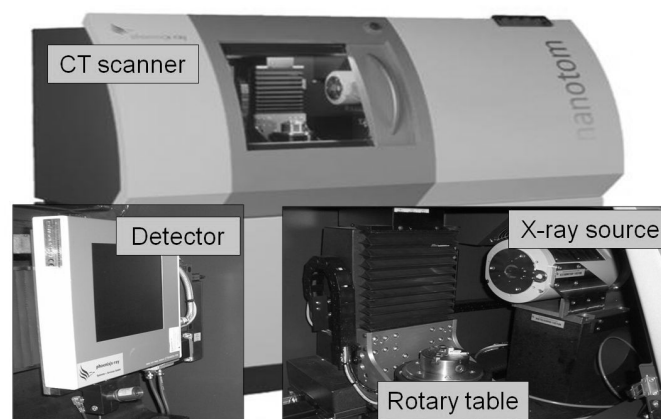


Figure 2.4: Industrial cone beam CT scanner [GE Phoenix X-ray Nanotom]

CT creates cross-section images by projecting a beam of emitted photons through one plane of an object from defined angle positions performing one revolution. As X-rays (emitted photons) pass through the object, some of them are absorbed, some are scattered, and some are transmitted. X Rays which are attenuated due to the interactions with the object do not

reach the X-ray detector. Photons transmitted through the object at each angle are collected on the detector and visualized by computer, creating a complete reconstruction of the scanned object. The 3D gray value data structure gained in this way represents the electron density distribution in the measured object. This density is the basis for the grayscale values we see in the generated CT images.

The project made use of Active Contouring for segmentation. Active contour is a type of segmentation technique which can be defined as, that makes use of energy forces and constraints for segregation of the pixels of interest from the image for further processing and analysis. Contour is a collection of points that undergoes interpolation process. The interpolation process can be linear, splines and polynomial which describes the curve in the image. The main application of active contours in image processing is to define smooth shape in the image and forms closed contour for the region. Active contour models involve snake model, gradient vector flow snake model, balloon model and geometric or geodesic contours. Active contours are used in various applications in the segmentation of the medical images. Different types of active contour models are used in various medical applications especially for the separation of required regions from the various medical images. Morphological Geodesic Active Contour model, is suitable for images with visible contours, even when contours might be noisy, cluttered, or partially unclear.

### 2.3 The summarized outcome of the literature review

Paper	Inference
<i>Tomazevic et al (2003)</i>	<p>This paper provided us some insight regarding Image Registration. The paper presented an image-registering approach for 3D CT or MR images to one or more 2D X-ray images.</p> <p>The registration is based solely on the information present in 2-D and 3-D images. It does not require fiducial markers, intraoperative X-ray image segmentation, or timely construction of digitally reconstructed radiographs.</p> <p>Registration of 2D x-ray images to 3D MRI data is a complex problem because of the difference in tissue contrasts between the data types. 2D–3D registration algorithms developed by Tomazevic show a significantly better performance in terms of accuracy and capture range when they are applied to CT instead of MRI data.</p>

<p><i>Van der Bom (2011)</i></p>	<p>The paper presents a p-CT generation technique that is based on a kNN-regression strategy that labels voxels of MRI data with CT Hounsfield Units.</p> <p>The regression method uses multiple sequences of MRI intensities and intensity gradients as features to discriminate between the various tissues.</p> <p>The author concluded that providing pseudo-CT data produced from MRI data could therefore improve the performance of the registration of x-ray images to MRI.</p>
<p><i>Uh J, Merchant TE (2011)</i></p>	<p>The authors suggested a study to assess the feasibility of the atlas registration approach for pCT generation. The method seemed feasible as it required only around 6 patient atlases to get a reasonable result. Also, it didn't require any major supervision like in the learning-based methods.</p> <p>The pseudo-CTs based on multiple atlases showed a high similarity to the real CTs and the corresponding calculated doses agreed well with those based on real CTs.</p>
<p><i>Mika Kapanen &amp; Mikko Tenhunen (2013)</i></p>	<p>The majority of the final implementation done in our project is based on this paper. This paper aimed to generate a method to convert bone MRI intensity into HU data.</p> <p>The HU conversion model was generated for 10 randomly chosen prostate cancer patients and independent validation was performed in another 10 patients. Data consisted of 800 image voxels chosen within the pelvic bones in both T1/T2*-weighted gradient echo and CT images. Relation between MRI intensity and electron density was derived from calibrated HU-values. The proposed method enables the generation of clinically relevant pseudo-CT data for the pelvic bones from one MRI series.</p> <p>It is simpler than previously reported approaches which require either acquisition of several MRI series or T2* maps with special imaging sequences. The method can be applied with</p>

	commercial clinical image processing software. The application requires segmentation of the bones in the MR images.
<i>Korhonen et al (2014)</i>	<p>T1/T2*-weighted MRI intensity values and standard computed tomography (CT) image HUs in the male pelvis were analyzed using image data of 10 prostate cancer patients.</p> <p>The data was utilized to generate a dual model HU conversion technique that converted bone segment local MRI intensity values to HU by applying a second-order polynomial model. This study complemented previous research by demonstrating that soft tissue electron density information in the male pelvis can be acquired accurately by relying on the data of a single MRI series.</p>
<i>Monnier (2014)</i>	<p>Current MR attenuation correction (AC) approaches suffer from the lack of precision in the detection of bone and the assigned attenuation coefficients. In general, no unique transformation of MR image intensities into attenuation coefficients exists.</p> <p>The purpose of this work was to derive attenuation coefficient maps from a single MR sequence via pseudo-CT map using a derived MRI-CT(HU) relationship. Even this method focussed on a polynomial-based strategy. However, they've utilized a Fuzzy Logic-based classifier first; before they parse the MR Intensities via the polynomial.</p>
<i>Han X. (2017)</i>	<p>The paper proposes a Deep Convolutional Neural Network (DCNN) based method for sCT generation which has 27 convolutional layers interleaved with pooling and unpooling layers and 35 million free parameters and evaluates its performance on a set of brain tumor patient images.</p> <p>Even though a deep neural network model typically requires a large amount of training data, very good performance is achieved with limited data by making use of an existing, pre-trained model through the principle of transfer learning.</p>

	<p>The DCNN method does not require any inter-subject image registration, either linear or deformable, and directly learns the mapping from the space of MR images to the corresponding CT images. Evaluation results showed that the DCNN method offered significantly better accuracy than an atlas-based method. The approach had to be discarded due to the unavailability of a sufficiently large amount of data.</p>
--	--

#### 2.4 Theoretical discussions

Most of the methods suggested in the Literature Review required multiple sequences of MRIs registered together to proceed further. The Atlas-based method was entirely dependent on the results of deformable registration of patient atlases. This implied that the required dataset must be big enough for generating any results. On the contrary, *Mika Kapanen & Mikko Tenhunen (2013)* gave a solution that required only a single sequence of MRIs for generating credible results. *Korhonen et al (2014)* was also based on the ideas suggested in *Mika Kapanen & Mikko Tenhunen (2013)*. *Monnier (2014)* also employed a polynomial-based strategy. Hence, we may conclude that a polynomial-based strategy might fetch a good result.

#### 2.5 General analysis

It may be argued that the polynomial given by *Mika Kapanen & Mikko Tenhunen (2013)* won't fetch good results unless perfect segmentation is performed to classify the target tissues for the polynomial suggested. One possible improvement may be to use an approach similar to *Monnier (2014)*, where a fuzzy logic-based classifier was made use of; and the soft tissues were treated using a different transformation. Also, using at least two to three pulse sequences for MRI (each patient in the dataset) can give clearer results. This is because there is no direct relation between MRI intensity values and CT Hounsfield Unit values as such, and there is surely no linear correlation between them either; Hence it always leaves the possibility of enhancing soft tissues in the pCT. If multiple sequences are accounted for per voxel then the inclusion of these additional parameters might change or reduce the previously occurring errors.

#### 2.6 Conclusions

A polynomial-based strategy seemed feasible for a trace amount of data; also its ease of implementation in real-time made it a good alternative. Hence, the core of the project was based on *Mika Kapanen & Mikko Tenhunen (2013)*.



## CHAPTER 3

### METHODOLOGY

#### 3.1 Overview

Our methodology is based on *Mika Kapanen & Mikko Tenhunen (2013)*, *Korhonen et al (2014)* and *Monnier (2014)*. These papers indicated a possible Polynomial relation between MR and CT intensity values. The method in *Mika Kapanen & Mikko Tenhunen (2013)* employs a Polynomial Function relating MRI Intensity values and CT-Hounsfield numbers based on a study conducted on the human pelvic region of 10 patients. The results of the paper indicated an AIC criteria value of two. Therefore, a second order was assumed for the polynomial in the method. Further emphasis must be given to the fact that a reference CT image wasn't provided for mapping the values. The method is solely based on Mathematical modeling due to the scarcity of data. Segmentation methods were employed to contain the reach of the polynomial sequence to only the bony structures.

#### 3.2 Methodology

The methodology can be broken into five steps. First, obtaining 2D slices for a given MRI DICOM Series. Second, abstracting matrix representations of generated slices. Each cell of a matrix corresponds to a pixel grayscale value. Third, generating modified images by employing the polynomial sequence with a correction factor. The mean value for the gaussian correction factor is based on the assumption that the provided series is of the Coronal or Frontal Plane to generalize the position of the spinal cord. Fourth, performing Morphological Geodesic Active Contouring on the modified images to generate masks. These masks are merged together by an OR-logic. Fifth, use the merged mask on the original image along with the polynomial sequence to get the final transformed image. A layout/block diagram depicting the general flow of the algorithms is provided in Figure 3.1.

Small solid fragments of bones generate susceptibility gradients within pores that are located next to them. These pores contain both water and fat. The gradients affect MRI intensity through changes in  $T2^*$ . The relationship is very complex and depends on the volume fraction of these solid parts, their number, thickness, and separation.

A simplified model generated by *Mika Kapanen & Mikko Tenhunen* gave a theoretical basis for the relationship between MRI intensity and HU-values. Signal intensity  $s$  in gradient echo imaging is given as  $s=A(T1) \cdot P \cdot \exp(-TE \cdot R2^*)$ , where  $R2^*=1/T2^*$ ,  $P$  is proton (spin) density and  $A$  is a  $T1$ -dependent factor determined by the flip angle,  $TR$  and level of spoiling of transverse magnetization. Time constant  $T1$  (longitudinal relaxation time) is a measure of the time taken for spinning protons to realign with the external magnetic field. Time Constant  $T2$  (transverse relaxation time) is a measure of the time taken for spinning protons to lose phase coherence among the nuclei spinning perpendicular to the main field.



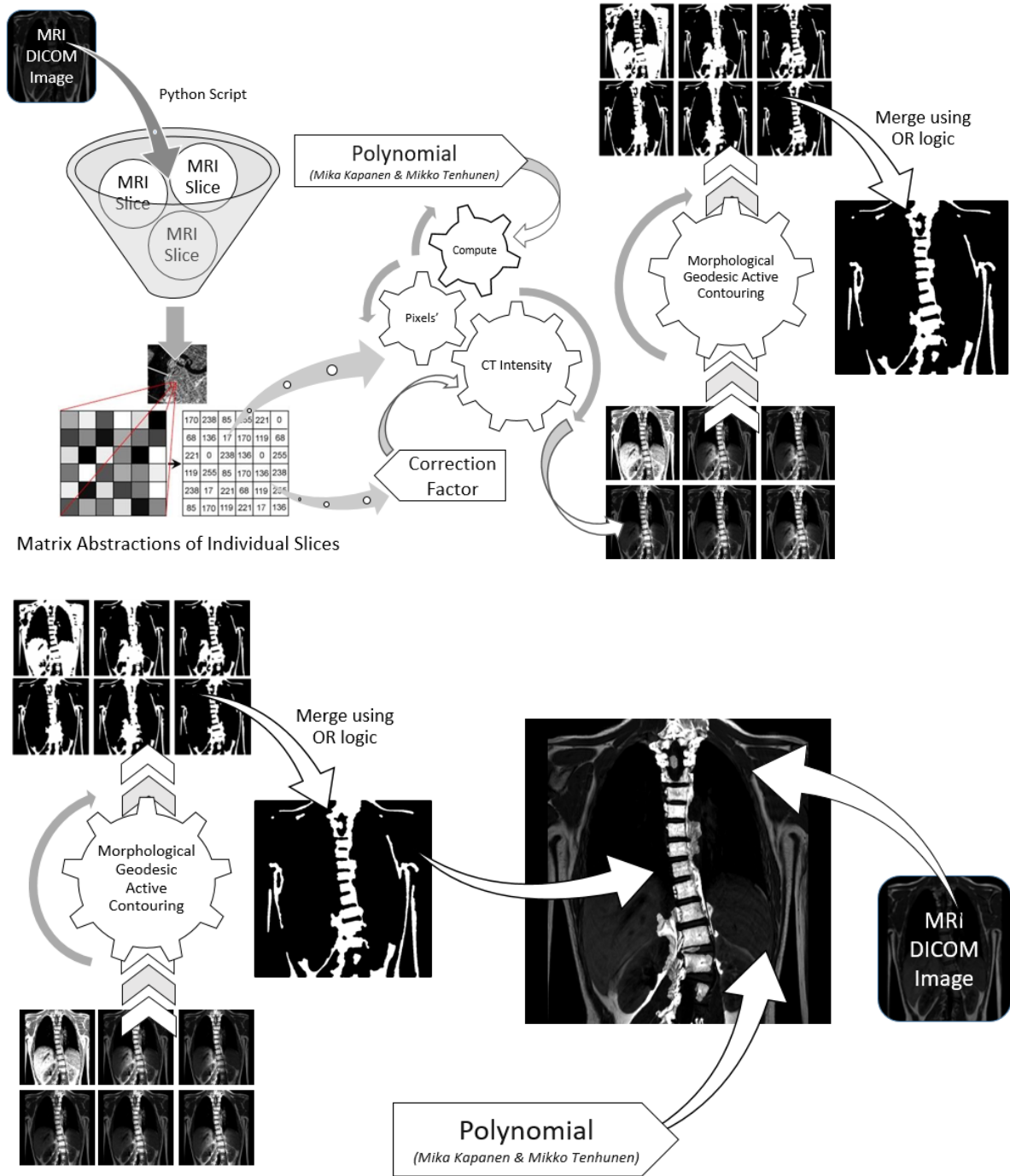


Figure 3.1: General Flow of the Program

Visible MRI signal comes from soft tissue components (such as collagen, collagen bound water, and pore water) and is integral over different values of T1, P and T2\* within a voxel. When normalizing to the signal from a muscle (water) we obtain the following equation:

$$s = \iiint \frac{A(T1(x, y, z))}{A_{\text{muscle}}} \frac{P(x, y, z)}{P_{\text{muscle}}} e^{-TE \cdot (R2^*(x, y, z) - R2^*_{\text{muscle}})} \rho(x, y, z) \cdot dx \cdot dy \cdot dz$$

Since mathematical forms of all the factors in the above equation are not known, the inversion was done by a series expansion which results in a simple polynomial model. The second-order polynomial fit is expressed as a solid line.

$$HU(s) \approx A + Bs + Cs^2$$

*Mika Kapanen & Mikko Tenhunen* concluded the following values A, B, and C are the fitting parameters and s is the MRI intensity value (normalized). The fitting parameters were A = 1947 (+/-71) HU, B = -11.39 (+/-0.79) HU/MRintensity unit and C = 0.0169 (+/-0.0022) HU/MR^2 intensity unit. The slope of a linear fit was -5.04 HU/MRintensity unit demonstrating a mean steepness of the non-linear fit as demonstrated in the graph below:

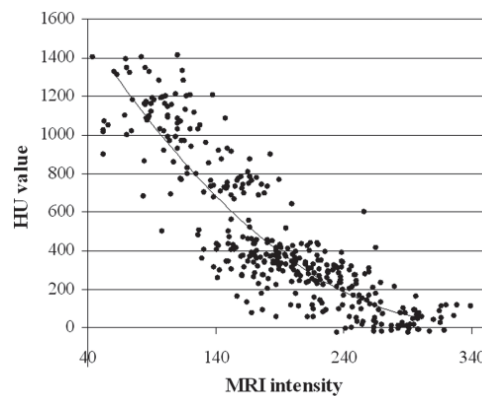


Figure 3.2: HU vs MRI intensity plot given by *Mika Kapanen & Mikko Tenhunen (2013)*

The polynomial was the crucial step in the methodology. It helped in acquiring the transformations for obtained matrix abstractions. The polynomial was multiplied by a Gaussian probability factor that modified the polynomial transformations depending on the likeliness of finding the spine in the region. Transformed matrices were converted to corresponding images.

### 3.3 Tools used

1. **Python:** Python is an interpreted, high-level, general-purpose programming language. Python's readability and along with the compatible libraries made it an apt choice.
2. **Jupyter Notebook:** It enabled proper organization of code snippets. It supports Python3. The shareability of the notebook made project management very convenient.
3. **Opencv library:** OpenCV is a library of programming functions mainly aimed at real-time computer vision. The library is cross-platform and free for use under the open-source Apache 2 License.
4. **Numpy library:** NumPy python library, adds support for large, multi-dimensional arrays and matrices, with a large collection of high-level mathematical functions to operate on these arrays. This was used for transformations of the matrix abstractions.

5. **Pydicom library:** *pydicom* is a pure Python package for working with DICOM files. It lets you read, modify and write DICOM data in an easy "pythonic" way.
6. **PIL library:** Python Imaging Library is a free and open-source additional library for the Python programming language that adds support for opening, manipulating, and saving many different image file formats. This was required for obtaining, displaying, and saving images from the transformed matrix abstractions.
7. **Imageio library:** Imageio provides an easy interface to read and write a wide range of image data, including animated images, volumetric data, and scientific formats.
8. **Math library:** This library was essential for certain mathematical functions.
9. **Morphsnakes library:** The Morphological Snakes are a family of methods for image-guided evolution of curves and surfaces represented as a level-set of an embedding function. They have application in several Computer Vision areas, such as image segmentation and tracking.
10. **Sklearn library:** Scikit-learn is a free software machine learning library for Python featuring classification, regression and clustering algorithms including *k*-means. It is designed to interoperate with numerical and scientific libraries NumPy and SciPy.
11. **Tensorflow library:** Open-source library for machine learning that can be used for a range of tasks but has a particular focus on training and inference of neural networks.
12. **Scipy Library:** SciPy is used for scientific computing and technical computing. It contains modules for optimization, linear algebra, integration, interpolation, special functions, signal processing, and other tasks common in science and engineering.
13. **RadiAnt Dicom Viewer:** The software can open and display studies obtained from different modalities. It was used for viewing and assessing the provided MRI image.

### 3.4 Preliminary result analysis

Image to Numpy Array executed [[0 0 0 ... 0 3 0] [0 0 0 ... 0 0 0] [0 0 0 ... 0 0 0] ... [0 0 0 ... 0 0 0] [0 0 0 ... 0 0 0] [0 0 0 ... 0 0 0]]	This result was obtained when png slices were passed through the <code>numpy_for_image</code> function. The corners of the image were mostly black. Hence, the obtained values at those points were near 0. This indicates that the transform is working fine.
Transformed Matrix to Image Synthesis completed [[ 0 0 0 0 ... 0 765 0] [ 0 0 0 0 ... 0 0 0] [ 0 0 0 0 ... 0 0 0] ... [ 0 0 0 0 ... 0 0 0] [ 0 0 0 0 ... 0 0 0] [ 0 0 0 0 ... 0 0 0]]	This output indicated that NumPy array was successfully parsed in the polynomial.  $\text{int}(1947*3 - 11.39*3 + 0.0169*3*3) > 765$ . This indicated that the correction factor can suppress intensities away from the spine.

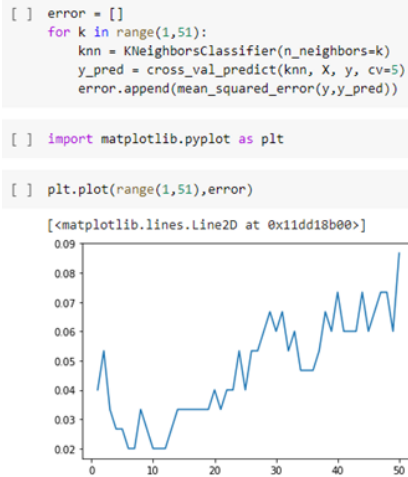
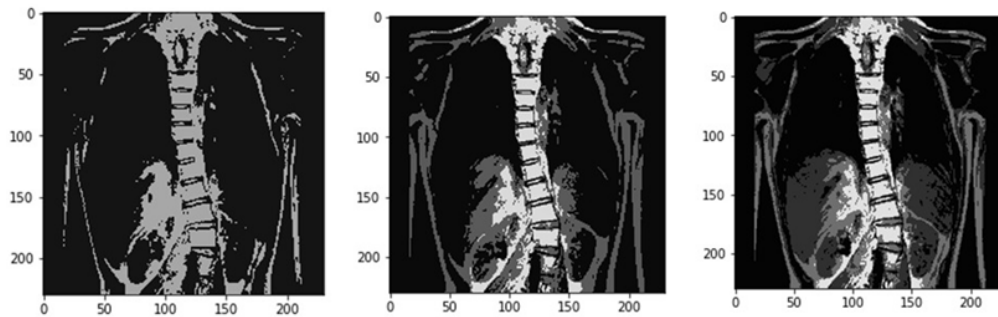
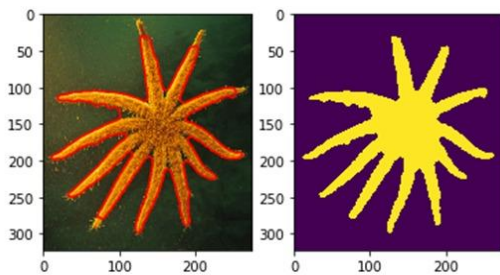


Figure 3.3: KNN Regressor Assessment

A test was run during the initial few months for checking the feasibility of the KNN Regressor Strategy. The test aimed at evaluating how many data points should be considered for a low mean-squared error and a reasonable  $r^2$  score. The same test was conducted on 2 different forms of simple data sets which were unrelated to Medical Imaging. However, we couldn't proceed with this method (mentioned in *Van der Bom 2011*) for pCT generation due to insufficient data.

Figure 3.4 Preliminary Results from K-Means Clustering  
(left to right for k=2,3,4 Respectively)

K-Means clustering is an unsupervised algorithm that partitions the unlabeled data into K parts based on K-centroids. The goal is to find groups based on some kind of similarity in the data with the number of groups represented by K. For the above case, the main objective was to check if this method can help in classifying the tissues for the preprocessing of images before they are fed for required transformations.

Figure 3.5 Morphological Geodesic  
Active Contour

Active Contour Model/Snakes, is a computer vision framework for delineating object outlines from noisy images. It is widely used for shape recognition and segmentation. It matches a deformable model to an image by means of energy minimization.

In Figure 3.5, an image of a starfish was tested, to generate feasible masks.

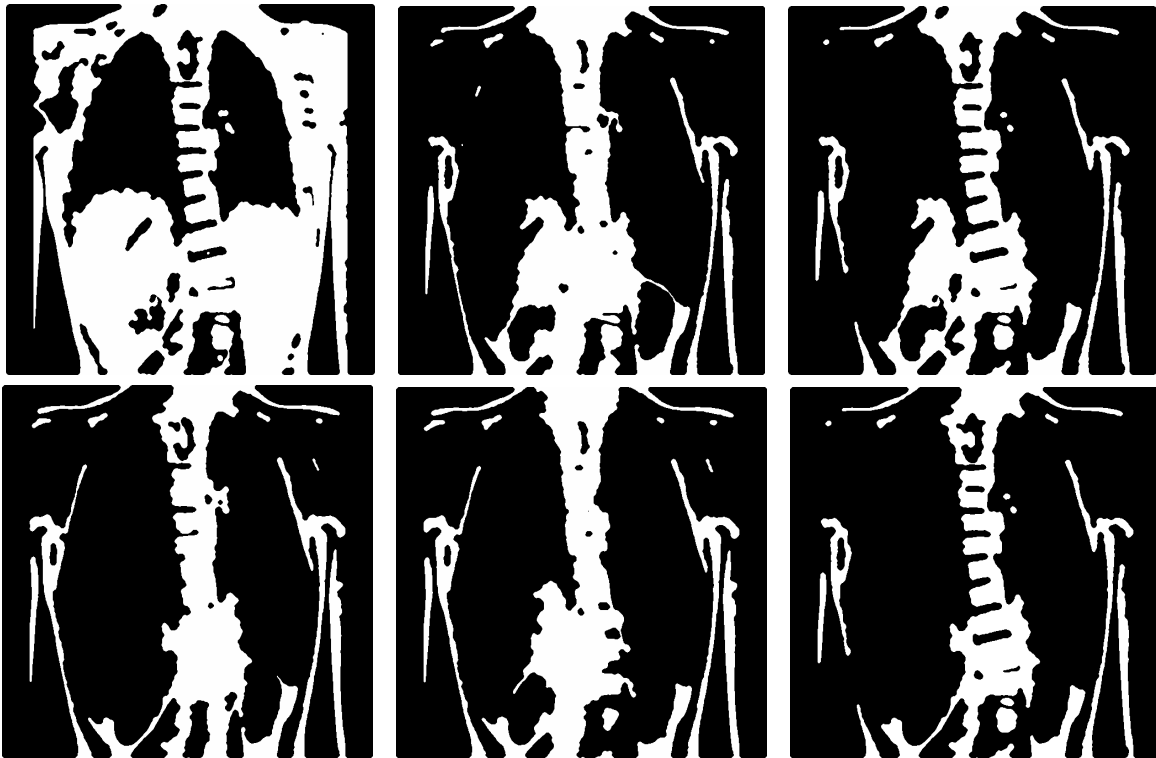


Figure 3.6

The above images are different masks generated for different Gaussian pdf (probability distribution function) parameters. All these masks merged via an or-logic to obtain the final mask as shown in Figure 4.8



Figure 3.7

The results obtained when the target polynomial was performed directly on the unmasked regions. This resulted in slight inaccuracies including skin tissues being regarded similar to the bony regions. Hence the gaussian correction factor was reinstated in the final step.

### 3.5 Conclusions

Different methods like KNN and CNN-based strategies were thoroughly studied and accordingly work had proceeded. However, due to the scanty dataset, the previous

methodologies based on learning-based algorithms were abandoned. Finally, a Polynomial based strategy based on *Mika Kapanen & Mikko Tenhunen (2013)* was selected. The method required only a single sequence of MRI which made it a better alternative than a 2D polynomial strategy as explained in *Korhonen et al (2014)*.

Moving further in the project, different python libraries were explored. Some of which were compatible with DICOM images. Various tools were employed and many papers were read. Apart from the procedure laid down in *Mika Kapanen & Mikko Tenhunen (2013)*, few novelties were added to limit the transformations only to the bony regions. Few Segmentation approaches were tried and tested with the objective of generating a mask that will limit the reach of the derived polynomial to only the bony regions.

Accordingly the hybrid (polynomial+correction factor) method was employed to generate many modified images by varying the mean and standard deviation values of the probability distribution function. These images were further used for generation of corresponding masks. The need for the mask arose from the fact that the tissues should be classified into bony and non-bony regions. In *Monnier (2014)*, a fuzzy logic based tissue classifier was used for differential transformations of the bony and soft tissues. However, the constraint for the given question was that the dataset was not big enough to train a model to classify tissues. Hence, various segmentation based methods were employed.

A single mask in the generated set did not match the required characteristics. However, each mask highlighted certain specific regions depending on the parameters of the pdf (see Figure 3.6). Hence, the masks were merged to generate a reliable mask (see Figure 4.8). The mask generated gave the target regions for the polynomial function.



## CHAPTER 4

### RESULT ANALYSIS

#### 4.1 Overview

After thorough analysis it was concluded that a polynomial based strategy would be the most effective for the provided dataset. The literature review suggested the same. To further improve the results, segmentation algorithms were tested to check if a suitable mask can be obtained to limit the polynomial based transformations to the bony regions. This chapter gives a brief explanation and justification for the final and intermediate results so obtained and tries to draw suitable conclusions from the same.

#### 4.2 Result analysis:



Result	Comments
 <p style="text-align: center;">Figure 4.1</p>	<p>Figure 4.1 shows the output generated when the polynomial transformation (<i>Mika Kapanen &amp; Mikko Tenhunen 2013</i>) is applied to the entire coronal MR slice. The result was thus concluded to be unreliable. For an accurate pCT image, only the bony regions should be distinctly visible. However, in Figure 4.1 even the soft tissues have been brightened. The reason for this is that the polynomial function extracted was applied to each pixel in the MRI image.</p>
 <p style="text-align: center;">Figure 4.2</p>	<p>To restrict the application of the polynomial function transformation to vertebrae/bony regions, a gaussian probability distribution function was used. The function was indicative of whether the pixel in question lies in the vertebrae region. Mean value for Gaussian distribution was kept at the middle of the x-axis with a standard deviation of 60. It was assumed that the vertebrae would occupy the middle pixels of the image. Figure 4.2 was obtained after accounting all these factors.</p>



Figure 4.3

Figure 4.3 was obtained after applying an unsharp mask on Figure 4.2. This was done to make the image look sharper.



Figure 4.4

Figure 4.4 uses similar methodology as Figure 4.2. Mean Value for the probability distribution function was kept as 10 units lower than the middle of the x-axis. Similar variations were generated with the objective of generating the masks to limit the reach of the polynomial sequence.

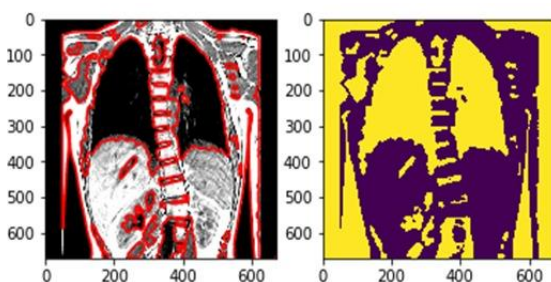


Figure 4.5

Morphological Geodesic Active Contouring performed on Figure 4.1, gave a mask given in Figure 4.5. Morphological Geodesic Active Contour is a type of segmentation algorithm which can generate a reliable mask that can be applied directly on MR image.

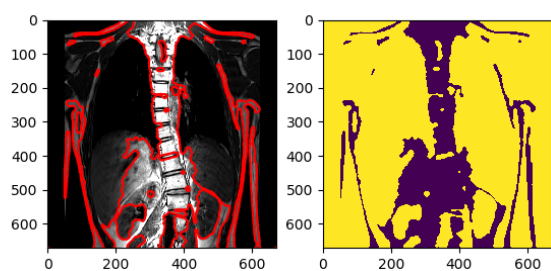


Figure 4.6

Morphological Geodesic Active Contouring performed on Figure 4.2, results in a mask displayed in Figure 4.6. This result was more reliable in comparison to the mask displayed in Figure 4.5.



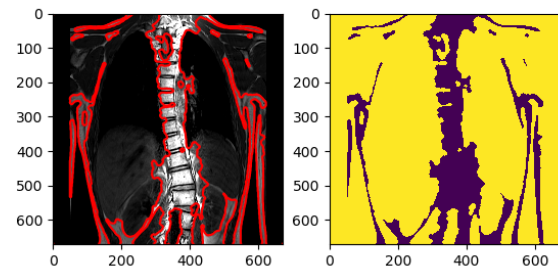


Figure 4.7

Morphological Geodesic Active Contouring performed on Figure 4.4, results in a mask displayed in Figure 4.7.

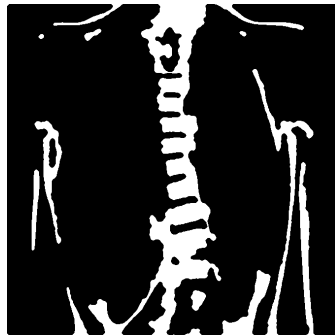


Figure 4.8

All the masks were converted to corresponding boolean matrices. The mask given in Figure 4.8 was obtained after merging all the generated masks by an OR-logic. The white areas are indicative of the regions where operation of the polynomial should be considered.



Figure 4.9

This Intermediate result was based on a preliminary mask. The result deviated from the expectations as regions of the lungs were also treated similarly to the bony regions.



Figure 4.10

Figure 4.10 shows the final result obtained after using the merged mask (Figure 4.8) on the experimental input MRI slice. The method was successfully able to segregate the vertebrae from the rest of the body. Accordingly the polynomial transformations were made only on the target regions.

### *4.3 Significance of the result obtained*

The final result obtained gave a real visual representation of the spinal region of the torso, but the adjacent bones like that of the shoulder bones were not visible in the final pCT obtained so it still will not find its usage in image-guided therapy. However, these results form a strong foundation for further development in the area.

### *4.4 Deviations from expected results & Justification*

The images obtained after running the proposed algorithm showed minor deviations compared to an actual CT image. The results provided insights for picking alternative approaches at various steps.

Reasons :

1. Unavailability of appropriate dataset was the major bottleneck. To employ any learning based methods or complex algorithms, the dataset should've consisted of multispectral MRI images registered along with CT images. However, finding scans for patients who've undergone therapy using both the modalities for a specific organ is very rare.
2. Tissue classification could not be performed due the miniscule dataset. An AI based tissue classifier can be used for segregating the bony structures from the soft tissues.
3. The assumption that the spinal cord occupies the middle portion of the image. Due to this assumption, nearby soft tissues may be brightened in the transformed image.
4. The transformations and segmentations were done considering individual MR slices. In reality the modalities are 3D and hence there is a need for considering values of adjacent cells in the upper and lower slices as well. However, that might make the program exponentially slower. Hence further work must be done to strike a balance between these two underlying problems.

### *4.5 Conclusions*

The results obtained became increasingly better after each modification. Also, it is noticeable that the images obtained were deviating from an actual CT image. It was expected that after an appropriate segmentation algorithm was applied to the original MR image, we'd be able to extract the bony tissues which might eventually improve the results. However, certain discrepancies from the true CT image remained intact. It can be attributed to many factors as stated in the previous section. Despite the contradictory results, some insightful data was generated which may be considered reasonable considering the small dataset.

## CHAPTER 5

### CONCLUSION AND FUTURE SCOPE OF WORK

#### *5.1 Brief summary of the work*

This project aimed to generate a pseudo-CT image from an MR image for the ease of registration with intraoperative X-ray images during image guided therapy. Working of the proposed algorithm can be understood as an integration of two main steps: the first one being able to find a proper transformation function and the other one is coming up with a mask that can accurately distinguish between different types of tissues. The major chunk of our work goes in creating a reliable mask that restricts the application of polynomial function, which transforms the MR intensity of the bony region into a CT Hounsfield number. Once these basic steps were accomplished the only thing left was manipulating the image matrix in order to get a required pCT.

#### *5.2 Conclusions*

After thorough study and analysis a polynomial-based strategy was adopted for the purpose of this work. However, it was found out that the bottleneck was how well the different tissues can be separated in the given MR image.

Results obtained improved with every modification. It may be noted that the pCT so generated deviated from an actual CT image. However, considering that a corresponding CT of the patient wasn't available, the result can be considered insightful for further work and development. The bony structures of the vertebrae were clearly identified by this novel algorithm. A better image can be generated if the appropriate dataset is abstracted and learning based methods are integrated with the project.

#### *5.3 Future scope of work*

One of the things that can be improved upon is the segmentation part. A few simple segmentation techniques were applied but with dissatisfactory results. These segmentation algorithms were not able to accurately extract all the bony structures. Morphological Geodesic Active Contour however did manage to highlight the vertebrae in the 2D slices; but it will not be able to display the bony structures hidden between soft tissues, i.e the bony tissue lying in upper or lower depths in the considered DICOM series.

The Preliminary masks were generated from the modified MRs assuming a sliding window of operation; based on the assumption that the mean of the gaussian correction factor is centered around the middle regions on the x axis. This negated the possibility of accounting the bony regions in the periphery of the operated slices. Hence, a better approach to segment the contents of the image slice must be considered. One possible solution for that would be to break image slices to multiple equally sized subparts and then run the proposed algorithm on

individual subparts to get associated masks and then recombine the subparts to generate the final image mask. This mask might prove more reliable but is still bound by speculation. Considering  $m$  divisions across each axis for sub-part generation; the time complexity of the program would multiply by  $m^2$  and this might come up as another challenge in pursuing this strategy as the time complexity is severely deteriorated.

Another area for improvement is integration of neural networks for the tissue classification step. For this purpose an appropriate dataset must be abstracted and in the training data the organs should be labeled under human supervision. Once the tissue classification conundrum is justified, abstracting data related to fat percentage of certain tissues might be helpful. This idea would be based more in consonance with *Monnier (2014)* than the one considered in this project based on *Mika Kapanen & Mikko Tenhunen (2013)*. A possible alternative may be a fuzzy logic-based classifier for differential transformations of soft tissues and bony tissues.

Also, the use of multiple pulse sequences for MRI for each patient in the dataset can fetch better results. This is because there is no direct relation between MRI intensity values and CT Hounsfield Unit values. There is surely no linear correlation between them either; hence, it always leaves the possibility of enhancing soft tissues in the pseudo-CT. If multiple sequences are accounted for per voxel then the inclusion of these additional variables might minimize the previous anomalies.

## REFERENCES

- [1] Han X. MR-based synthetic CT generation using a deep convolutional neural network method. *Med Phys*. 2017;44(4):1408–19.
- [2]. Van der Bom, M. J.; Pluim, J. P. W.; Gounis, M. J.; van de Kraats, E. B.; Sprinkhuizen, S. M.; Timmer, J.; Homan, R.; Bartels, L. W. Registration of 2D x-ray Images to 3D MRI by Generating Pseudo-CT Data. *Phys. Med. Biol.* 2011, 56, 1031–1043
- [3] Uh J, Merchant TE, Li Y, Li X, Hua C. MRI-based treatment planning with pseudo CT generated through atlas registration. *Med Phys*. 2014 May;41(5):051711. doi: 10.1118/1.4873315. PMID: 24784377; PMCID: PMC5148041.
- [4] Mika Kapanen & Mikko Tenhunen (2013) T1/T2\*-weighted MRI provides clinically relevant pseudo-CT density data for the pelvic bones in MRI-only based radiotherapy treatment planning, *Acta Oncologica*, 52:3, 612-618, DOI: [10.3109/0284186X.2012.692883](https://doi.org/10.3109/0284186X.2012.692883).
- [5] Korhonen, J., Kapanen, M., Keyriläinen, J., Seppälä, T. and Tenhunen, M. (2014), A dual model HU conversion from MRI intensity values within and outside of bone segment for MRI-based radiotherapy treatment planning of prostate cancer. *Med. Phys.*, 41: 011704. <https://doi.org/10.1118/1.4842575>
- [6] Tomazevic, Dejan & Likar, Bostjan & Slivnik, Tomaz & Pernus, Franjo. (2003). 3-D/2-D registration of CT and MR to X-ray images. *IEEE transactions on medical imaging*. 22. 1407-16. 10.1109/TMI.2003.819277.
- [7] Monnier F, Fayad H, Bert J, Lapuyade-Lahorgue J, Hatt M, Veit-Haibach P, Delso G, Visvikis D. Generation of pseudo-CT from a single MRI for PET/MR attenuation correction purposes. *EJNMMI Phys*. 2014 Jul;1(Suppl 1):A74. doi: 10.1186/2197-7364-1-S1-A74. PMID: 26501665; PMCID: PMC4545960.
- [8] Sjölund, Jens & Forsberg, Daniel & Andersson, M & Knutsson, Hans. (2015). Generating patient specific pseudo-CT of the head from MR using atlas-based regression. *Physics in medicine and biology*. 60. 825-839. 10.1088/0031-9155/60/2/825.
- [9] Liu F, Yadav P, Baschnagel AM, McMillan AB. MR-based treatment planning in radiation therapy using a deep learning approach. *J Appl Clin Med Phys*. 2019 Mar;20(3):105-114. doi: 10.1002/acm2.12554. PMID: 30861275; PMCID: PMC6414148.
- [10] Gary Liney, Uulke van der Heide, “MRI for Radiotherapy”, Springer International Publishing, Edition Number - 1, ISBN number : 978-3-030-14441-8

## PROJECT DETAILS

<b><i>Student Details</i></b>			
<b>Student Name</b>	<b>Shivam Kumar Sharma</b>		
Register Number	170907044	Section / Roll No	A/10
Email Address	shivam.kumar@learner.manipal.edu	Phone No (M)	8002002763
<b>Student Name</b>	<b>Hritvik Kishore</b>		
Register Number	170907150	Section / Roll No	D/28
Email Address	hritvik.kishore@learner.manipal.edu	Phone No (M)	9741392577
<b><i>Project Details</i></b>			
<b>Project Title</b>	<b>Generation of Pseudo-CT Image from MRI of Spine</b>		
Project Duration	4 Months	Date of reporting	11/01/2021
Expected date of completion	07/05/2021		
<b><i>Organization Details</i></b>			
<b>Organization Name</b>	<b>Manipal Institute of Technology</b>		
Full postal address	Udupi - Karkala Rd, Eshwar Nagar, Manipal, Karnataka 576104		
Website address	<a href="https://manipal.edu/mit.html">https://manipal.edu/mit.html</a>		
<b><i>Supervisor Details</i></b>			
Supervisor Name			
Designation			
Full postal address			
Email address		Phone No (M)	
<b><i>Internal Guide Details</i></b>			
<b>Faculty Name</b>	<b>Dr. Anitha H.</b>		
Full postal address	Dept. of E&C Engg., Manipal Institute of Technology, Manipal – 576104 (Karnataka State), INDIA		
Email address	anitha.h@manipal.edu		